

RESEARCH

Open Access



Link of TMPRSS2 expression with tumor immunogenicity and response to immune checkpoint inhibitors in cancers

Karthikeyan Subbarayan^{1†}, Helena Bieber^{1†}, Chiara Massa², Felipe Adonis Escalona Rodríguez^{1,3,4}, SM Al Amin Hossain¹, Lisa Neuder¹, Wafa Wahbi⁵, Tuula Salo^{5,6}, Sandy Tretbar⁷, Ahmed Al-Samadi^{5,8} and Barbara Seliger^{1,2,7*} 

Abstract

Background SARS-CoV-2 and other viruses rely on the protease function of the TMPRSS2 protein to invade host cells. Despite cancer patients often experience poorer outcomes following SARS-CoV-2 infection, the role of TMPRSS2 in different cancer types has not yet been analyzed in detail. Therefore, the aim of the study was to determine the expression, function and clinical relevance of TMPRSS2 in tumors.

Methods Publicly accessible RNA sequencing data from tumors, adjacent tissues and whole blood samples of COVID-19 patients as well as data from human tumor epithelial and endothelial cells infected with SARS-CoV-2 were analyzed for TMPRSS2 expression and correlated to the expression of immune-relevant genes and clinical parameters. In vitro models of cells transfected with TMPRSS2 (TMPRSS2^{high}), siTMPRSS2 or mock controls (TMPRSS2^{low} cells) were analyzed by qPCR, flow cytometry, ELISA and Western blot for the expression of immune response-relevant molecules. Co-cultures of TMPRSS2 model systems with blood peripheral mononuclear cells were employed to evaluate immune cell migration, cytotoxicity and cytokine release.

Results Higher expression levels of TMPRSS2 were found in blood from patients infected with SARS-CoV-2, while TMPRSS2 expression levels significantly varied between the tumor types analyzed. TMPRSS2^{high} tumor cells exhibit increased activity of the interferon (IFN) signal pathway accompanied by an increased expression of class I human leukocyte antigens (HLA-I) and programmed cell death ligand 1 (PD-L1) elevated interleukin 6 (IL-6) secretion and reduced NK cell-mediated cytotoxicity compared to TMPRSS2^{low} mock controls. Treatment with a Janus kinase (JAK) 2 inhibitor or TMPRSS2-specific siRNA decreased TMPRSS2 expression. Co-cultures of the in vitro TMPRSS2 models with peripheral blood mononuclear cells in the presence of the immune checkpoint inhibitor nivolumab resulted in a significantly increased migration and infiltration of immune cells towards TMPRSS2^{high} cells and a reduced release of the innate immunity-related cytokines CCL2 and CCL3.

[†]Karthikeyan Subbarayan and Helena Bieber contributed equally to this work.

*Correspondence:
Barbara Seliger
barbara.seliger@uk-halle.de

Full list of author information is available at the end of the article



Conclusions This study provides novel insights into the role of TMPRSS2 in various tumor systems and the impact of SARS-CoV-2 infection on the host immunogenicity via the activation of immune-relevant pathways. These findings were linked to the efficacy of immune checkpoint inhibitor therapy, offering a potential alternative strategy to mitigate the severity of COVID-19.

Keywords SARS-CoV-2, TMPRSS2, Immune escape, Immune response, Tumors

Background

Coronavirus disease 2019 (COVID-19) has rapidly emerged as a global health pandemic mediated by infection with the severe acute respiratory syndrome coronavirus 2 (SARS-CoV-2). The virus utilizes the angiotensin-converting enzyme 2 (ACE2) receptor for its cellular entry and the transmembrane protease serine 2 (TMPRSS2) for the priming of the spike (S) protein [1]. Since some coronaviruses, such as SARS-CoV-1, MERS-CoV, and SARS-CoV-2, are activated by TMPRSS2 [2], there is an urgent need for the development of broad anti-viral strategies targeting multiple coronaviruses by focusing on common elements, such as TMPRSS2 and ACE2. In this context, TMPRSS2 inhibitors have been shown to block viral infections [3] suggesting their use as a potential therapeutic approach [4, 5].

Moreover, there exists growing evidence that tumor patients have an increased risk of COVID-19 infection and are more susceptible to severe illness with a worse outcome [6–12]. So far, there exists only limited information about the link between the expression of immune-relevant molecules in cancer patients, susceptibility to SARS-CoV-2 infection and the severity of the disease [13]. For example, an upregulation of the programmed cell death ligand (PD-L)1 expression during the cytokine storm of SARS-CoV-2-infection has been detected [14], but also infections with other viruses have been shown to upregulate PD-L1 expression, leading to immune escape [14, 15]. Consequently, PD-L1/PD-1 immune checkpoint inhibitor (ICPi) therapy might represent a potential treatment option to enable T cells to combat cancer cells [16], while controlling SARS-CoV-2 infection.

Under physiological conditions, TMPRSS2 is expressed in various tissues, including pancreas, prostate, stomach, kidney, small intestine as well as the respiratory tract, which is a primary site of SARS-CoV-2 infection [17]. The TMPRSS2 expression in pan-tissues is associated with pathways involved in immune metabolism, cell growth as well as stromal and cancer signatures [18]. During pathological conditions, the TMPRSS2 expression levels and their prognostic value highly varied across different cancer types [17]. For example, TMPRSS2 levels are elevated in prostate cancer [19], but decreased in colon cancer when compared to corresponding normal tissues [17]. Furthermore, the expression of TMPRSS2 in lung adenocarcinoma is linked to a positive prognosis, while

it is associated with a negative prognosis in breast cancer [20].

Cancer patients may have a higher mortality rate due to a COVID-19-mediated hyperinflammatory state, which is accompanied by severe disease manifestations [8, 14]. In severe cases, virus spread is linked to excessive IL-6 production associated with severe inflammation and tissue damage, while this response is controlled in mild cases [14, 21]. In contrast, IL-2 has the potential to improve the immune response to COVID-19 but is also a key factor in disease severity due to its involvement in cytokine release and immune regulation [22].

The JAK-STAT pathway is a fundamental signaling mechanism involved in anti-viral and anti-tumoral immune responses [23], but also involved in the hyperinflammatory response occurring in severe COVID-19 cases [24]. However, the impact of SARS-CoV-2-associated molecules, including TMPRSS2, on the JAK-STAT signal transduction has not yet been determined. Therefore, an increased understanding of the functions and interactions of TMPRSS2 with the JAK-STAT pathway and their regulated molecules, such as class I human leukocyte antigens (HLA-I) and PD-L1, is urgently needed and might provide insights into their potential as therapeutic targets thereby enhancing the patients' outcomes by improving the management of COVID-19.

Consequently, this study aims to elucidate the expression patterns and clinical significance of TMPRSS2 across different cancer types by analyzing publicly available RNA sequencing data, to assess in vivo immunological pathways associated with varying TMPRSS2 expression levels and to explore how their dynamics might affect the outcome of SARS-CoV-2-infected cancer patients. These results will provide insights into potential therapeutic approaches, including immune checkpoint inhibitors (ICPi), to improve the management of cancer patients during emerging and re-emerging coronavirus outbreaks.

Methods

Cell culture and transfections

The human tumor epithelial cell lines MCF-7 (breast cancer (BC)), MDA-MB-468 (BC) and the endothelial cell line EA.Hy926 were obtained from the American Type Culture Collection (ATCC, Manassas, USA). All cell lines were grown in RPMI1640 medium with the exception of EA.Hy926, which was cultured in DMEM/F12. The culture mediums were supplemented with 2 mM

L-glutamine, 10% fetal calf serum (FCS, PAN-Biotech, Aidenbach, Germany) and appropriate antibiotics.

Cell lines were transfected with the TMPRSS2 expression vector, designated as TMPRSS2^{high} (Addgene, Watertown, USA), using the Effectene Transfection Reagent (Qiagen, Hilden, Germany) according to the manufacturer's instructions. A control was established using a mock vector, referred to as TMPRSS2^{low/mock}.

Lipid nanoparticles (LNPs) were formulated by mixing lipid stock solutions in ethanol, composed of D-Lin-MC3-DMA, DPPC, Cholesterol, and PEG-DMG in a molar ratio of 50:10:35:5. These were combined with either a siTMPRSS2 or negative control (Thermo Fisher, Waltham, USA), utilizing an amine-to-phosphate (N/P) ratio of 3.1, which corresponds to 0.054 µg of nucleic acid per µmol of total lipid. Subsequently, the LNP complex was used to transfect the TMPRSS2^{high} MDA-MB-468 cells, resulting in the generation of TMPRSS2-silenced cells.

RNA extraction and real-time quantitative RT-PCR

Cellular RNA was extracted using the NucleoSpin RNA II kit (Macherey-Nagel, Düren, Germany). 2 µg RNA/sample was converted into cDNA using the Revert H Minus First Strand cDNA synthesis kit (Fermentas, Thermo Fisher) and oligo(dT)18 primer following the manufacturer's instructions. Utilizing a standard laboratory protocol, qRT-PCR was conducted on a Bio-Rad CFX96 system (Bio-Rad, Hercules, USA) with the platinum SYBRGreen qPCR Supermix UDG (Thermo Fisher) as described [25] using primers directed against HLA-I, APM components, IFN signaling molecules, PD-L1 and TMPRSS2-regulated genes (Supplementary Table 1). Data were evaluated using the comparative quantification mode of the CFX Maestro Software 2.3 (Bio-Rad) and presented as a mean of a minimum of three independent experiments.

Western blot analysis

For Western blot analysis, 30 µg protein/sample was separated by SDS-PAGE and then transferred using the iBlot™ 2 Dry Blotting System (Invitrogen, Thermo Fisher) prior to staining with antibodies (Abs) specific to TMPRSS2, IFI27 and STAT1 (Cell Signaling Technology, Danvers, USA). To ensure equal protein loading, the blot was stained with a monoclonal antibody (mAb) against ACTB (Cell Signaling Technology, Danvers, USA). A horse-reddish peroxidase (HRP) conjugated secondary Ab was applied before visualizing the proteins using an ECL-based system for chemiluminescence.

Flow cytometry

Flow cytometry was conducted as recently described [26]. The antibodies employed for flow cytometry were

HLA-I and PD-L1 mAbs (Invitrogen, Waltham, USA). Briefly, tumor cells were labeled with the appropriate amounts of antibodies at 4 °C in darkness for 30 min. HLA-I and PD-L1 expression was assessed on a NAVIOS flow cytometer (Beckman Coulter, Brea, USA) and data was analyzed using the Kaluza Software. The results were presented as mean fluorescence intensity (MFI) from at least three independent experiments.

Quantification of IL-6 by ELISA

To quantify IL-6 in TMPRSS2^{low} and TMPRSS2^{high} EA.Hy926 cells, the supernatants were collected, and the amount of IL-6 produced by the endothelial cells was calculated using an ELISA (LEGENDplex™ Macrophage/Microglia Panel, BioLegend) following the manufacturer's instructions. Data acquisition was conducted using the BD Symphony A3, and analysis was performed with the LEGENDplex™ Data Analysis Software Suite.

mRNA sequencing and data analyses

RNA sequencing was performed on the Illumina Novaseq 6000 platform by Novogene (Cambridge, United Kingdom). The reference genome and gene model annotation files were obtained from the genome website (NCBI/UCSC/Ensembl). HTSeq v0.6.1 was used to quantify gene expression levels, and the FPKM of each gene was calculated based on the gene's length and the mapped read counts [27]. The initial analysis of differential gene expression (DGE) between TMPRSS2^{low} and TMPRSS2^{high} MCF7 and EA.Hy926 cells using the DESeq2 R package (2.1.6.3) was conducted by Novogene (Munich, Germany). The p-values were adjusted using Benjamini and Hochberg's approach to control the False Discovery Rate (FDR). Genes with an adjusted p-value (Padj) < 0.05 in DESeq2 data were identified as differentially expressed. The differentially expressed genes (DEGs) were subjected to Gene Ontology (GO) and Kyoto Encyclopedia of Genes and Genomes (KEGG) enrichment analyses using the clusterProfiler (v4.0.5) R package. KEGG terms with corrected Padj value < 0.05 were considered significantly enriched.

Microfluidic chip assay

TMPRSS2^{high} and TMPRSS2^{low} MCF-7 cells were labeled with CellTrace™ Far Red (Invitrogen, Thermo Fisher) according to the manufacturer's instructions for microfluidic chip tests and then suspended in RPMI1640-based myogel/fibrin gel derived from human tumors containing 2.4 mg/ml myogel, 0.5 mg/ml fibrinogen (Merck, Darmstadt, Germany), 33.3 µg/ml aprotinin (Sigma-Aldrich) and 0.3 U/ml thrombin (Sigma-Aldrich) as well as 5 µM of IncuCyte caspase-3/7 green (Sartorius, Göttingen, Germany) to identify apoptotic cells. The TMPRSS2^{high} and TMPRSS2^{low} MCF-7 cells were then divided into a

control group without drug and a group treated with 0.5 μM nivolumab (Opvido[®], Selleckchem, Houston, Texas, USA). Subsequently, 2 μL of cell suspension (i.e., 500 cells) were loaded into separate small “cancer cell channels” of the microfluidic chip as previously described [28].

Peripheral blood mononuclear cells (PBMNCs) purified by gradient density centrifugation from the buffy coats of healthy donors provided by the Finnish Red Cross were stained with CellTrace™ Violet (Invitrogen) following the manufacturer’s instructions. Cell viability and number were assessed using trypan blue staining with CellCountess (Invitrogen). After staining, the cells were suspended in cell culture media supplemented with 10 ng/ml of recombinant human IL-2 (BioLegend, San Diego, California, USA) and 5 μM caspase-3/7 green (Sartorius). The PBMNCs were then divided into a control group without drug and a group treated with 0.5 μM nivolumab. Subsequently, 1×10^5 viable PBMNCs in 100 μL was added to the larger ‘PBMNC channels’ of the chip as previously described [28]. In controls without PBMNCs, 100 μL of cell culture media containing 5 μM caspase-3/7 green was injected.

Following the injections, the chips were placed in a cell culture incubator and incubated for 72 h with daily imaging conducted using a Nikon Ti-E with Alveole Primo microscope (Nikon, Tokyo, Japan) connected to a Hamamatsu Orca Flash 4.0 LT B&W camera (Hamamatsu Photonics, Hamamatsu, Japan). The conditioned medium was then collected from the chips and stored at -80°C until further use.

Cytokine profiling

The Abcam FirePlex Service (Boston, USA) was used to perform cytokine profiling on the conditioned media from the microfluidic chips with a FirePlex[®]-96 Key Cytokines (Human) Immunoassay Panel (Abcam, Cambridge, UK). This panel can detect 17 cytokines, including the granulocyte-macrophage colony-stimulating factor (CSF2, GM-CSF), IL-1B, IL-2, IL-4, IL-5, IL-6, IL-9, IL-10, IL-12 A, IL-13 and IL-17 A, CXCL8, IFN γ , monocyte chemoattractant protein-1 (MCP-1, CCL2), macrophage inflammatory protein 1 alpha (MIP1- α , CCL3), macrophage inflammatory protein 1 beta (MIP1- β , CCL4) and tumor necrosis factor (TNF)- α . Each sample was analyzed in duplicate.

NK cell activity

Human PBMNCs were activated for 18 h using 1 ng/ml of IL-12, 5 ng/ml of IL-15 (Immunotools, Friesoythe, Germany) and 50 ng/ml of IL-18 (Biovision, Milpitas, CA, USA) in X-vivo15 medium (Lonza). Subsequently, the cells were co-cultured with TMPRSS2^{high} and TMPRSS2^{low} target cells at a ratio of 1:1 followed by degranulation

assay. Briefly, an anti-CD107a antibody was added for 1 h to the co-culture before the cells were stained with monoclonal antibodies (mAbs) against CD3, CD16 and CD56 (BioLegend) after 4 h to identify NK cells and assess overall NK cell activity.

Multi-dataset analysis of transcriptomic and genomic data

Transcriptomic data from 24 healthy controls and 62 COVID-19 patients [29, 30] were examined using COVID19db (ID: COVID000010). Previously published characteristics of the patients, such as age, gender and blood parameters, were referenced [29]. Data from Calu3 cells, a lung adenocarcinoma cell line infected with SARS-CoV-2, was obtained from GEO: GSE147507. Metadata from a cohort of SARS-CoV-2 and other respiratory viruses, including human parainfluenza virus 3 (HPIV3), respiratory syncytial virus (RSV), mutant influenza A virus (IAVdNS) infected cells as well as COVID-19 positive lung biopsies (GEO accession: GSE147507) were analyzed using ImmGen of Immunological Genome Project [31–33]. Single-cell RNA-seq data of peripheral blood from patients with severe COVID-19 were obtained from ImmGen [34]. Additional datasets were obtained from the Gene Expression Omnibus (GEO), which included the following: an organoid model infected with the SARS-CoV-2 Alpha variant (B.1.1.7) (GEO: GSE178333), samples from patients experiencing long COVID-19-a condition marked by persistent symptoms following SARS-CoV-2 infection (GEO: GSE224615; [35]) and samples from C57BL/6J wild-type mice infected with SARS-CoV-2 (GEO: GSE253635; [36]). The expression of the TMPRSS2 transcript across different tumor types and their corresponding normal tissues was analyzed using The Cancer Genome Atlas (TCGA) datasets through UALCAN [37, 38]. Metadata from a cohort of BC ($n=782$) and lung cancer ($n=91$) cases obtained from TCGA (portal: <https://portal.gdc.cancer.gov>) [39] and GEO dataset (GSE18842) were analyzed using the R2: Genomics analysis and visualization platform (<http://r2.amc.nl>). The gene expression patterns of TMPRSS2, HLA class I APM, IFN pathway components and PD-L1 were extracted from the datasets.

Statistical analysis

The graphical presentations, Student’s t-test and one-way ANOVA were conducted using Microsoft Excel-Office 365, BioRender and R (RStudio 3.0). Analysis of cytokine release was performed using the FirePlex™ Analysis Workbench software (<https://www.abcam.com/kits/fireplex-analysis-workbench-software>). A p -value < 0.05 was considered statistically significant (*, $p < 0.05$; **, $p < 0.01$; ***, $p < 0.001$).

Results

High levels of TMPRSS2 expression following SARS-CoV-2 infection

RNAseq data from PBMCs collected from 24 healthy individuals and 62 COVID-19 patients (COVID19db ID: COVID000010) revealed increased levels of TMPRSS2 mRNA in PBMCs after SARS-CoV-2 infection (Fig. 1A). This increase was comparable to the TMPRSS2 mRNA levels observed in SARS-CoV-2-infected Calu3 lung carcinoma cells (Fig. 1B). Analyses of TCGA datasets showed a heterogeneous expression of TMPRSS2 across different cancer types. When compared to corresponding normal tissue, higher mRNA expression levels of TMPRSS2 were found in BLCA, CESC, KICH, PRAD and UCEC, lower in BRCA, COAD, HNSC, KIRC, KIRP, LIHC, LUAD, LUSC and READ whereas TMPRSS2 expression was unchanged in CHOL, ESCA, GBM, PAAD, PCPG, SARC, SKCM, THCA, THYM and STAD (Fig. 1C).

Influence of TMPRSS2 overexpression on transcriptomic profiles

To determine the effect of TMPRSS2 on the gene expression pattern, MCF-7 and EA.Hy926 were transfected with a TMPRSS2 expression vector. Global transcriptomic profiles obtained after RNA sequencing of TMPRSS2^{high} vs. TMPRSS2^{low} MCF-7 cells and EA.Hy926 demonstrated 4452 and 1949 DEGs in MCF-7 and EA.Hy926 cells, respectively. Among these DEGs, 2061 genes were upregulated and 2391 genes were downregulated in TMPRSS2^{high} MCF-7 (Supplementary Fig. 1A), while 1108 genes were upregulated and 841 genes were downregulated in TMPRSS2^{high} EA.Hy926 (Supplementary Fig. 1B). Analyses of the top 30 upregulated and downregulated genes revealed 11 commonly upregulated genes (IFI6, TMPRSS2, IFIT1, IFIT2, IFIT3, OAS2, OASL, HLA-B, ISG15, LGALS3BP and IFI44L) and only one commonly downregulated gene (PRR11) in the two cell lines. The commonly upregulated genes of the in vitro models were also upregulated in COVID-19 vs. healthy PBMCs, as highlighted in the Volcano plot (Fig. 2A). The KEGG terms retrieved from COVID19db (Fig. 2B) and the DEGs in TMPRSS2^{high}

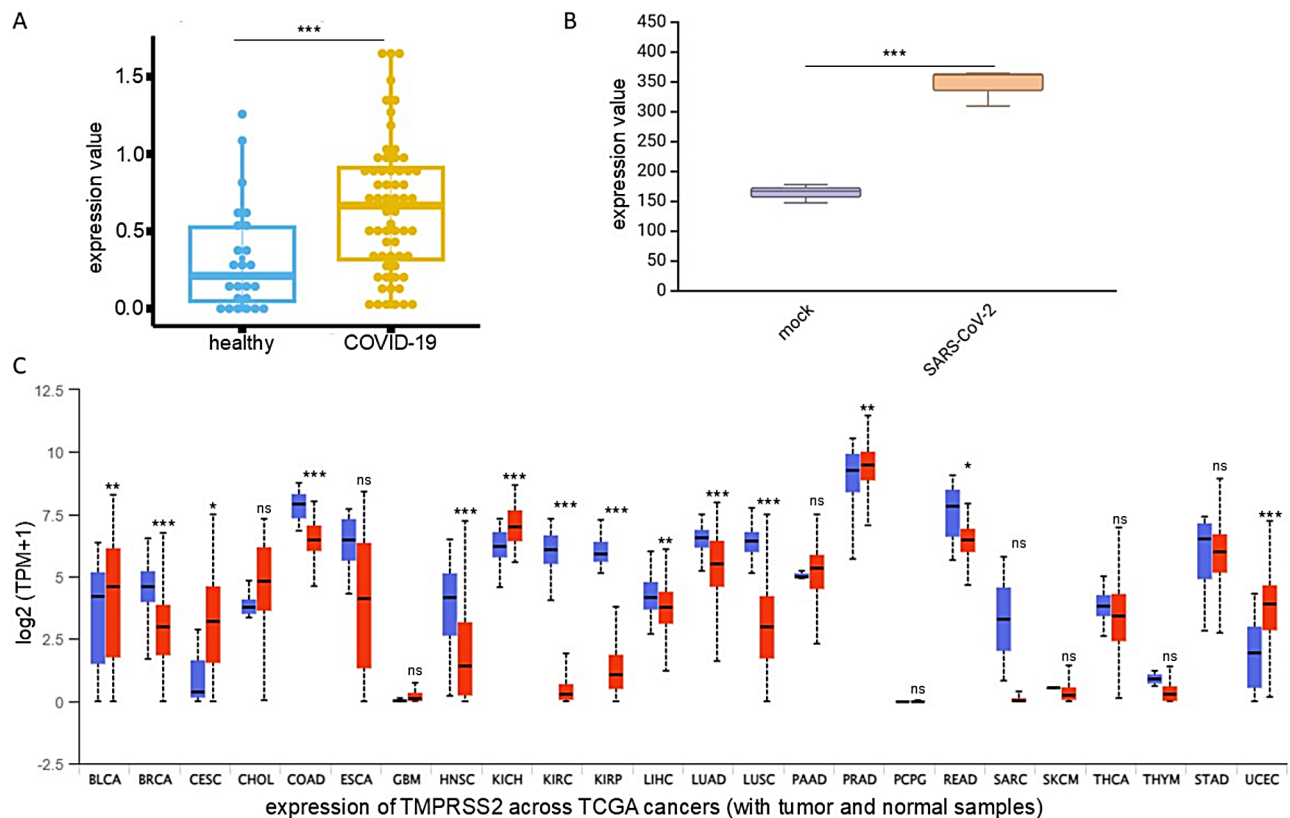


Fig. 1 Increased levels of TMPRSS2 expression in blood samples from COVID-19 patients and in cell lines infected with SARS-CoV-2 compared to uninfected controls. **A:** TMPRSS2 expression levels were analyzed in blood samples from 24 healthy individuals and 62 patients with COVID-19. These data were obtained from whole blood transcriptomics analyses (COVID19db). **B:** TMPRSS2 expression in Calu3 lung carcinoma epithelial cells was evaluated after infection with SARS-CoV-2 (GEO: GSE147507). **C:** The TMPRSS2 transcriptomic expression across various tumor types (red bars) and their adjacent normal tissues (blue bars) was examined using TCGA datasets. The results are displayed in a bar chart. t.test, ns: $p > 0.05$; *: $p \leq 0.05$; **: $p \leq 0.01$; ***: $p \leq 0.001$

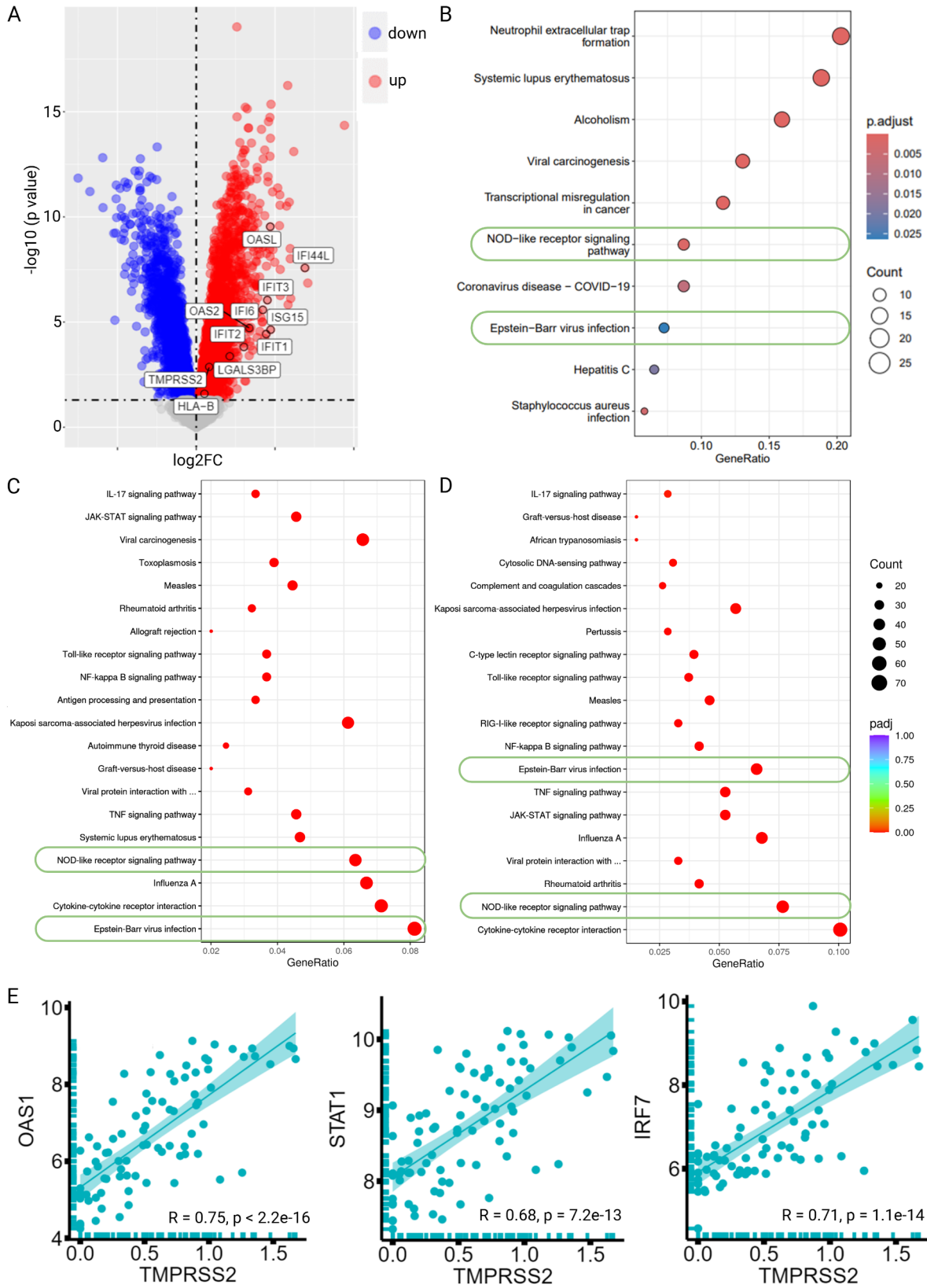


Fig. 2 (See legend on next page.)

(See figure on previous page.)

Fig. 2 An analysis of transcriptional profiles and KEGG pathway enrichments in COVID-19 vs. healthy PBMNCs along with TMPRSS2^{high} versus TMPRSS2^{low} MCF-7 and EA.Hy926 cells were conducted using RNA sequencing. **A:** A Volcano plot depicts the differentially expressed genes (DEGs) between COVID-19 and healthy blood samples (COVID19db). Genes that are significantly downregulated are indicated in dark blue, while significantly upregulated genes are shown in red and non-significantly regulated genes are represented in grey. **B:** The top 10 enriched KEGG pathways from the upregulated genes between COVID-19 and healthy blood samples are presented. **C, D:** The top 20 enriched KEGG terms derived from the upregulated genes of TMPRSS2^{high} versus TMPRSS2^{low} MCF-7 (**C**) and EA.Hy926 (**D**) cells are displayed. The enriched GO terms found in both TMPRSS2^{high} and COVID-19 are highlighted with green circles. **E:** Correlation plots illustrate the commonly upregulated genes in the two most enriched KEGG pathways concerning TMPRSS2 expression from blood samples of COVID-19 patients (COVID19db). The gene expressions of OAS1, STAT1 and IRF7 are exemplified here

MCF-7 (Fig. 2C) and EA.Hy926 (Fig. 2D) showed that Epstein-Barr virus infection and the NOD-like receptor signaling pathway were similarly enriched across all three settings: TMPRSS2^{high} MCF-7, TMPRSS2^{high} EA.Hy926, and COVID-19 PBMNCs. In addition, within these KEGG terms, there were 12 commonly upregulated genes, namely OAS2, OAS1, OAS3, STAT1, TNFAIP3, IRF7, STAT2, NFKBIA, IFNB1, MYD88, IRF9 and IL-6. Correlation plots between TMPRSS2 and commonly upregulated genes were representatively shown for OAS1, STAT1 and IRF7 from COVID-19 vs. healthy PBMNCs (Fig. 2E). In contrast, no common KEGG terms were found in downregulated DEGs between TMPRSS2 transfectants of MCF-7 and EA.Hy926 and PBMNCs of COVID-19 patients (Supplementary Fig. 2). To expand the analysis, the upregulated genes identified in our cell culture system (MCF-7 and EA.Hy926 cells) were further investigated in an organoid model infected with the SARS-CoV-2 alpha variant (B.1.1.7) (GEO: GSE178333) and in patients with long COVID-19, a condition characterized by post-acute sequelae following SARS-CoV-2 infection (GEO: GSE224615; [35]). As shown in Supplementary Table 2, genes associated with the IFN pathway, such as IFI27, IFIT1, IFIT2, OASL and OAS3, showed significantly higher expression levels, in particular individuals with long COVID-19 when compared to non-long COVID-19 and the organoid systems infected with the alpha variant.

Impact of TMPRSS2 on HLA-I expression, IFN signaling and NK cell recognition

Since the RNAseq data revealed an increased expression of IFN signaling genes in TMPRSS2^{high} vs. TMPRSS2^{low} cells, the impact of TMPRSS2 on the expression of HLA-I surface antigens was determined in MCF-7 and EA.Hy926 cells by flow cytometry. As shown in Fig. 3A, overexpression of TMPRSS2 resulted in an upregulation of HLA-I surface antigens, which could be correlated to enhanced mRNA expression of major components of the antigen processing machinery (APM) such as the transporter associated with antigen processing (TAP)1, TAP2 and TAPBP were upregulated by TMPRSS2 overexpression (Fig. 3B). As expected, the TMPRSS2-mediated HLA-I upregulation had also an impact on NK cell responses. Using a CD107 degranulation assay, a

reduced NK cell recognition of TMPRSS2^{high} compared to TMPRSS2^{low} MCF-7 cells was identified (Fig. 3C).

Based on the KEGG pathway enrichment analysis, different JAK-STAT signaling molecules, as well as IFN pathway genes, were also investigated in TMPRSS2^{high} vs. TMPRSS2^{low} tumor cells. A significant increase in the mRNA expression of IRF1, IRF9, STAT1, STAT2 and STING in TMPRSS2^{high} transfectants compared to the TMPRSS2^{low} mock controls was found (Fig. 3D). The TMPRSS2-mediated altered mRNA levels were accompanied by increased protein levels as representatively shown for IRF1, IFI27, STAT1, pSTAT1 and STAT2 in TMPRSS2^{high} vs. TMPRSS2^{low} cells (Fig. 3E).

The link between TMPRSS2 expression and immune response-relevant profiles was further validated by in silico analyses of cancer genome databases with a positive correlation between TMPRSS2 and the expression of HLA-I APM and IFN type I and II pathway genes (Supplementary Table 3).

TMPRSS2-mediated upregulation of ACE2 expression

To investigate whether there is an interplay between TMPRSS2 and ACE2, the key entry point for SARS-CoV-2 into cells (Fig. 4A), the ACE2 expression was determined in TMPRSS2^{high} vs. TMPRSS2^{low} cells. TMPRSS2^{high} EA.Hy926 cells exhibited higher protein levels of ACE2 (Fig. 4B) compared to TMPRSS2^{low} cells, suggesting a connection between TMPRSS2 and ACE2 expression in these cells. Furthermore, a correlation analysis of COVID-19 and healthy PBMNCs revealed a potential association ($r=0.24$; $p=0.026$) between TMPRSS2 and ACE2 (Fig. 4C). The upregulation of ACE2 by TMPRSS2 in cancer cells and PBMNCs highlights a significant overlap between cancer biology and infectious diseases, particularly in the context of the COVID-19 pandemic.

Link of TMPRSS2 overexpression with PD-L1 surface expression

Since TMPRSS2 plays a significant role in immune activation and exhaustion, the expression levels of inhibitory checkpoint molecules, including PD-L1 (CD274), PD-1 (PDCD1), CTLA4 and several others (specifically ADORA2A, ADORA2B, BTLA, CYBB, HAVCR2, IDO1, LAG3, SIGLEC7, VTCN1 and CD276) was analyzed upon SARS-CoV-2 infection and TMPRSS2 overexpression

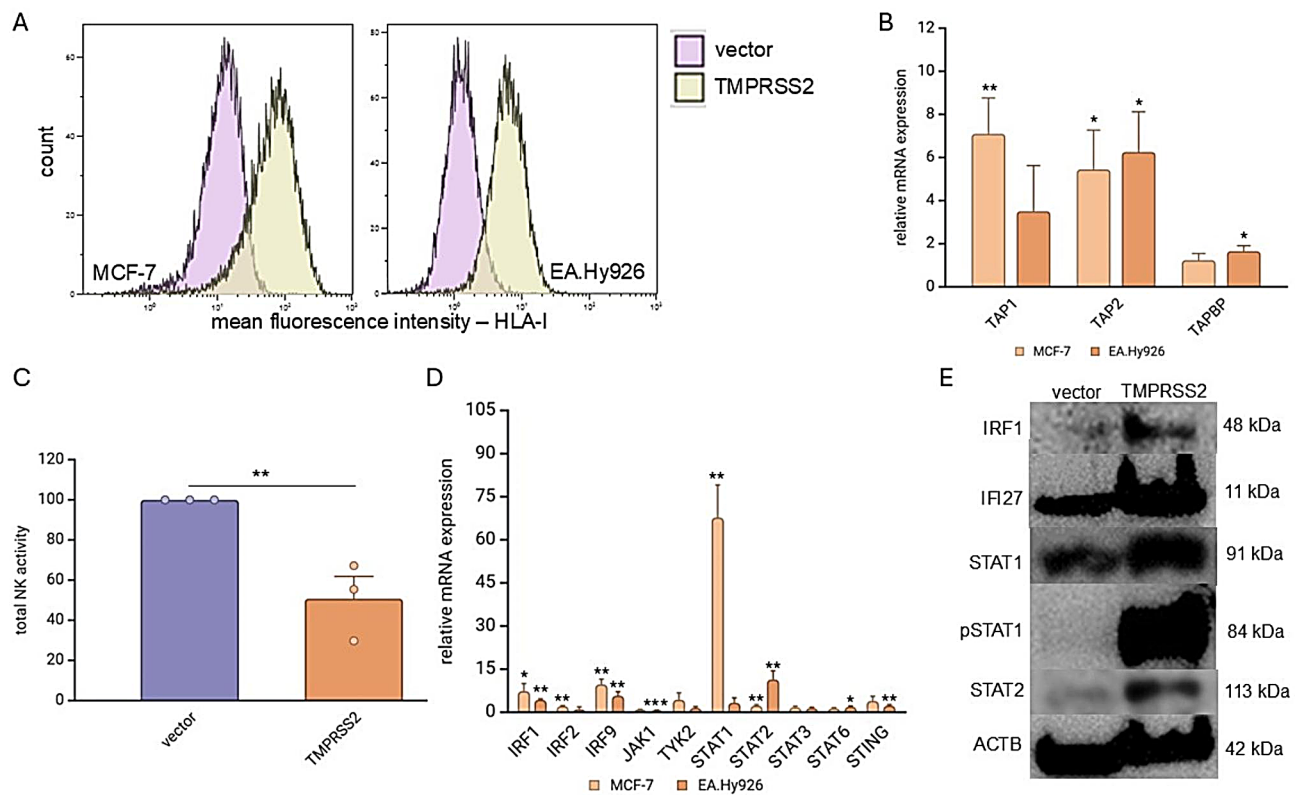


Fig. 3 Effects of TMPRSS2 overexpression on HLA class I expression, the antigen presentation machinery (APM) and interferon (IFN) signaling in TMPRSS2-transfected cells and their influence on natural killer (NK) cell function. **A:** Flow cytometry was used to assess HLA-I surface expression in TMPRSS2 transfectants and mock control MCF-7 and EA.Hy926 cells as described in the Methods. The results are displayed as a histograms with the mean fluorescence intensity (MFI) of HLA-ABC ($n=3$). **B:** The expression of major HLA-I APM components in TMPRSS2 transfectants was evaluated using qPCR as described in the Methods. **C:** The cytotoxic activity of NK cells from three different donors against TMPRSS2^{low} and TMPRSS2^{high} MCF-7 cells was evaluated using a CD107a degranulation assay. Data are shown as mean \pm SE of CD107a degranulation upon normalization to the mock-transfected cells. **D:** TMPRSS2 transfectants were examined by qPCR for the expression of components of the IFN as well as JAK-STAT signaling pathways. The results are shown as an x-fold induction in the expression of these signaling components in TMPRSS2 transfectants relative to mock controls. **E:** Representative Western blot analyses of TMPRSS2^{high} and mock-transfected using antibodies directed against IRF1, IRF27, STAT1, pSTAT1 and STAT2. Staining with an anti-ACTB antibody served as a loading control

(Supplementary Table 4). High levels of PD-L1 and IDO1 were found in SARS-CoV-2-infected in vitro, Calu3 cells and in vivo mouse models. These data were in line with transcriptomic analyses of TMPRSS2^{high} MCF-7 and EA.Hy926 cells demonstrated a marked increase in the expression of PD-L1 and IDO1. Furthermore, elevated PD-L1 levels in COVID-19 patients were closely linked to high mortality rates [14]. TMPRSS2^{high} MCF-7 and EA.Hy926 cells exhibited higher levels of PD-L1 mRNA and protein expression compared to TMPRSS2^{low} control cells. This was determined through qPCR (Fig. 5A), Western blot analysis (data not shown), and flow cytometry (Fig. 5B). The increased PD-L1 levels in TMPRSS2-transfected tumor cells were further supported by in silico data (COVID19db ID: COVID000010). A correlation analysis between TMPRSS2 and PD-L1 in peripheral blood mononuclear cells (PBMCs) from COVID-19 patients and healthy controls (Fig. 5C) revealed a positive correlation ($R=0.54$; $p=7.2e-08$). These data suggest that

the TMPRSS2^{high} cells partially resemble COVID-19 disease conditions and postulate ICPi as a treatment option.

Increased secretion of IL-6 upon TMPRSS2 overexpression

IL-6 has been identified as the primary driver of the cytokine storm [40]. Our analysis revealed that elevated IL-6 levels were found in the supernatants of TMPRSS2^{high} cells compared to the TMPRSS2^{low} EA.Hy926 cells (Fig. 5D). These data were confirmed by in vivo mouse lung data obtained from GEO ID: GSE253635 with significantly enhanced IL-6 levels in C57BL6/J wild-type mice following SARS-CoV-2 infection [36]. Additionally, high IL-6 levels were found in PBMC samples from patients with long COVID-19 (GEO: GSE224615; [35]) compared to uninfected PBMCs. In addition to IL-6, 15 other cytokines, chemokines, and growth factors were analyzed to provide a comprehensive overview of the inflammatory response induced by SARS-CoV-2. These include CSF2, IL-2, IL-4, IL-5, IL-1 β , IL-9, IL-10, IL-12 A,

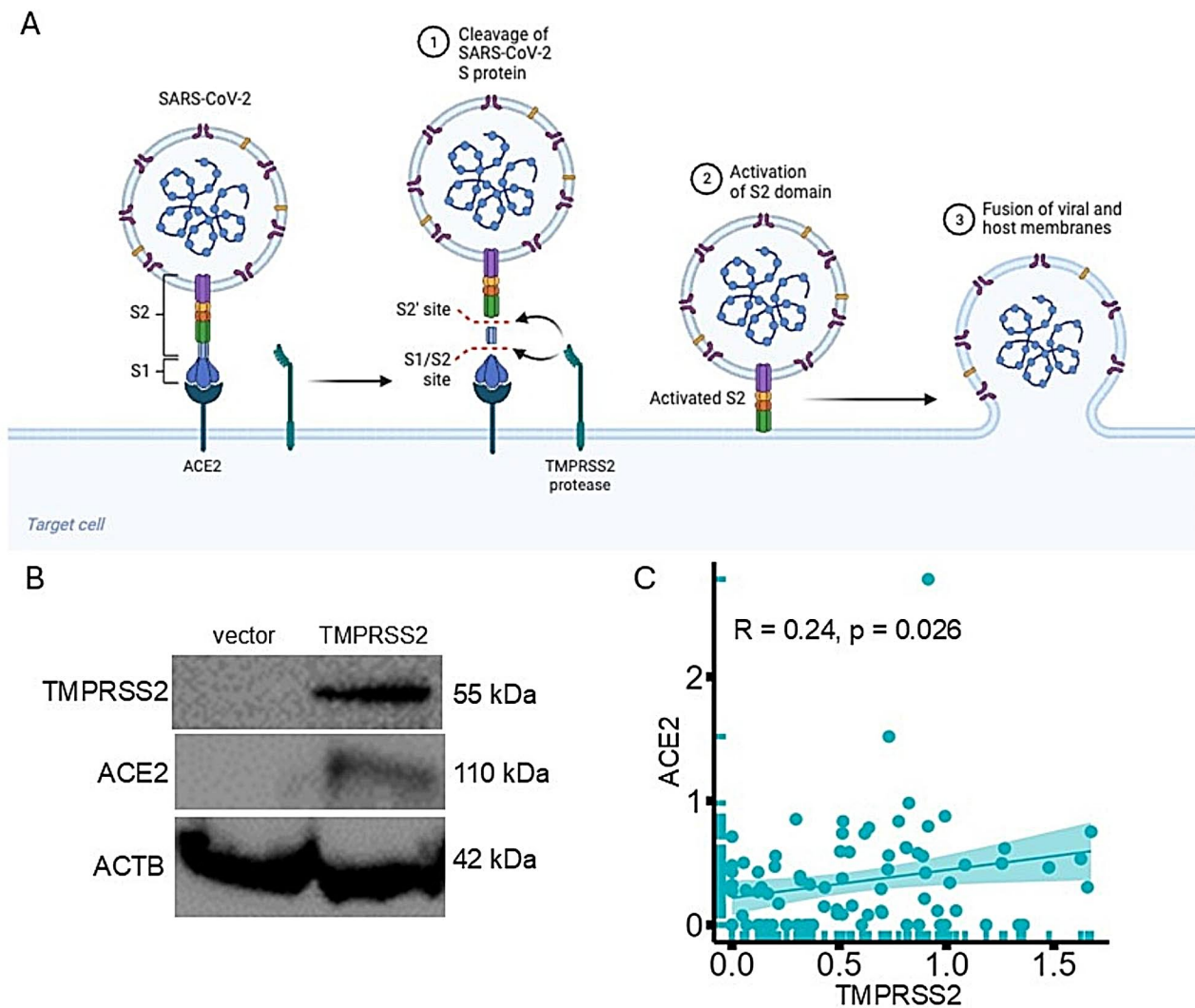


Fig. 4 TMPRSS2-mediated upregulation of ACE2 expression. **A:** ACE2 serves as a receptor for the entry of SARS-CoV-2, while TMPRSS2 is involved in the activation of the spike (S) protein. These are crucial elements for comprehending the pathophysiology of COVID-19. **B:** ACE2 expression of TMPRSS2^{high} and mock-transfected EA.Hy926 cells was determined by Western blot using an anti-ACE2 as well as anti-TMPRSS2 mAb. **C:** A correlation plot illustrates the association of ACE2 and TMPRSS2 expression in PBMCs of COVID-19 patients (COVID-19db)

IL-13, IL-17 A, IFN- γ , CCL2, CCL3, CCL4, and TNF (Supplementary Table 5). Following SARS-CoV-2 infection, C57BL6/J mice exhibited increased levels of CCL2, IFN- γ , IL-10, IL-1 β and IL-6.

Suppression of TMPRSS2 expression by a JAK2 inhibitor and small interfering RNA

Based on the SARS-CoV-2-mediated induction of IFN pathway components, TMPRSS2^{high} MDA-MB-468 cells were treated with the JAK2 inhibitor ruxolitinib [41]. Ruxolitinib reduced JAK2 levels (data not shown) and decreased TMPRSS2 and ACE2 protein expression (Fig. 6A). Using a dataset from MCF-7 cells (GEO dataset ID: GSE21618), positive correlations of TMPRSS2 gene expression with these of JAK1 (Fig. 6B; $R=0.684$;

$p=4.88e-21$) and JAK2 (Fig. 6C; $R=1.99$; $p=0.017$) were found via the R2 genomics platform.

To further explore the role of TMPRSS2, silencing experiments were conducted using siTMPRSS2. As expected, transfection with the siTMPRSS2-LNP complex decreased the TMPRSS2 protein levels in TMPRSS2^{high} MDA-MB-468 cells (Fig. 6D). This significant downregulation of TMPRSS2 correlated with a decrease of both HLA-I (Fig. 6E) and PD-L1 (Fig. 6F) surface expression, confirming a crucial role of TMPRSS2 in the modulation of both molecules (Fig. 5C).

Increased immune cell migration of TMPRSS2^{high} vs. TMPRSS2^{low} MCF-7 cells after treatment with nivolumab

In the context of COVID-19, blocking the PD-1 pathway has been shown to counteract the immune system

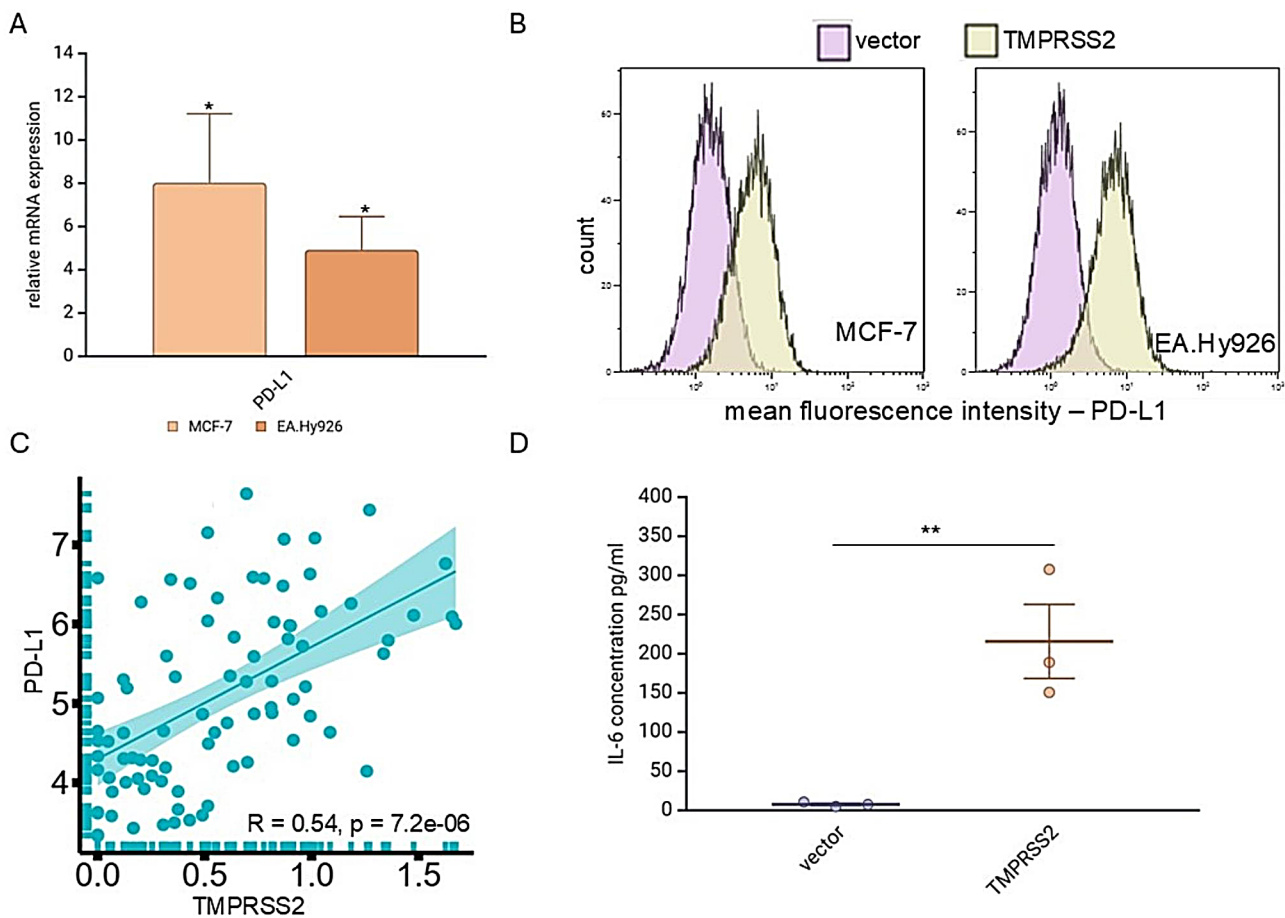


Fig. 5 Enhanced PD-L1 and IL6 expression in TMPRSS2^{high} cells. **A:** mRNA expression by qPCR analysis was performed to assess the expression levels of PD-L1 in both TMPRSS2^{high} cells and mock-transfected control cells. **B:** Flow cytometry was used to evaluate PD-L1 surface expression in TMPRSS2 transfectants of MCF-7 and EA.Hy926 cells ($n = 3$). The results are presented as MFI. **C:** A correlation plot depicts the relationship between TMPRSS2 and PD-L1 expression in blood samples from COVID-19 patients (COVID-19db). **D:** The supernatants from TMPRSS2^{high} and TMPRSS2^{low} EA.Hy926 cells were assessed for IL-6 secretion using ELISA. The data represents the mean from three independent experiments

abnormalities induced by the virus and enhance the body's immune response against SARS-CoV-2 [42]. To investigate whether the expression levels of TMPRSS2 may influence the efficacy of anti-PD1 mAb treatments, the immune cell migration, cancer cell proliferation and apoptosis were determined over three days of co-cultures between TMPRSS2^{low} or TMPRSS2^{high} MCF-7 and immune cells in the presence and absence of nivolumab. The immunofluorescent images captured throughout the three-day time frame post-nivolumab treatment revealed a nivolumab-mediated significant increase of the immune cell infiltration towards the TMPRSS2^{high} MCF-7 cells (Fig. 7A), but only a marginal movement of immune cells towards TMPRSS2^{mock/low} MCF-7 cells (Fig. 7B). Representative immunofluorescent images post-nivolumab treatment from immune cells targeting TMPRSS2^{high} (Fig. 7C) and TMPRSS2^{low} cells (Fig. 7D) on day 3 were shown. Additionally, the nivolumab treatment has slightly increased apoptosis rates of TMPRSS2^{high} than TMPRSS2^{low} MCF-7 cells (Fig. 7E). The nivolumab-mediated

inhibition of PD-L1 on TMPRSS2^{high} MCF-7 cells might lead to increased immune cell infiltration and facilitate T cell activation. These data suggest the therapeutic potential of this treatment in redirecting the immune response against these cancer cells.

Link of altered cytokine release and TMPRSS2 expression upon nivolumab treatment

The impact of nivolumab on the cytokine release in the cell supernatants during the co-culture of PBMCs with TMPRSS2^{high} and TMPRSS2^{low} MCF-7 cells was investigated using a human FirePlex[®]-96 key cytokine immunoassay panel. As shown in Fig. 7E, treatment of TMPRSS2^{high} and TMPRSS2^{low} MCF-7 cells with nivolumab decreased the release of CCL2 and CCL3. However, there was an increase in IL-2 secretion in the TMPRSS2^{high} cells compared to the TMPRSS2^{low} cells. It's important to note that IL-2 was added during the experiment, which may have influenced its secretion. The elevated IL-6 secretion (Fig. 5E) was slightly but not

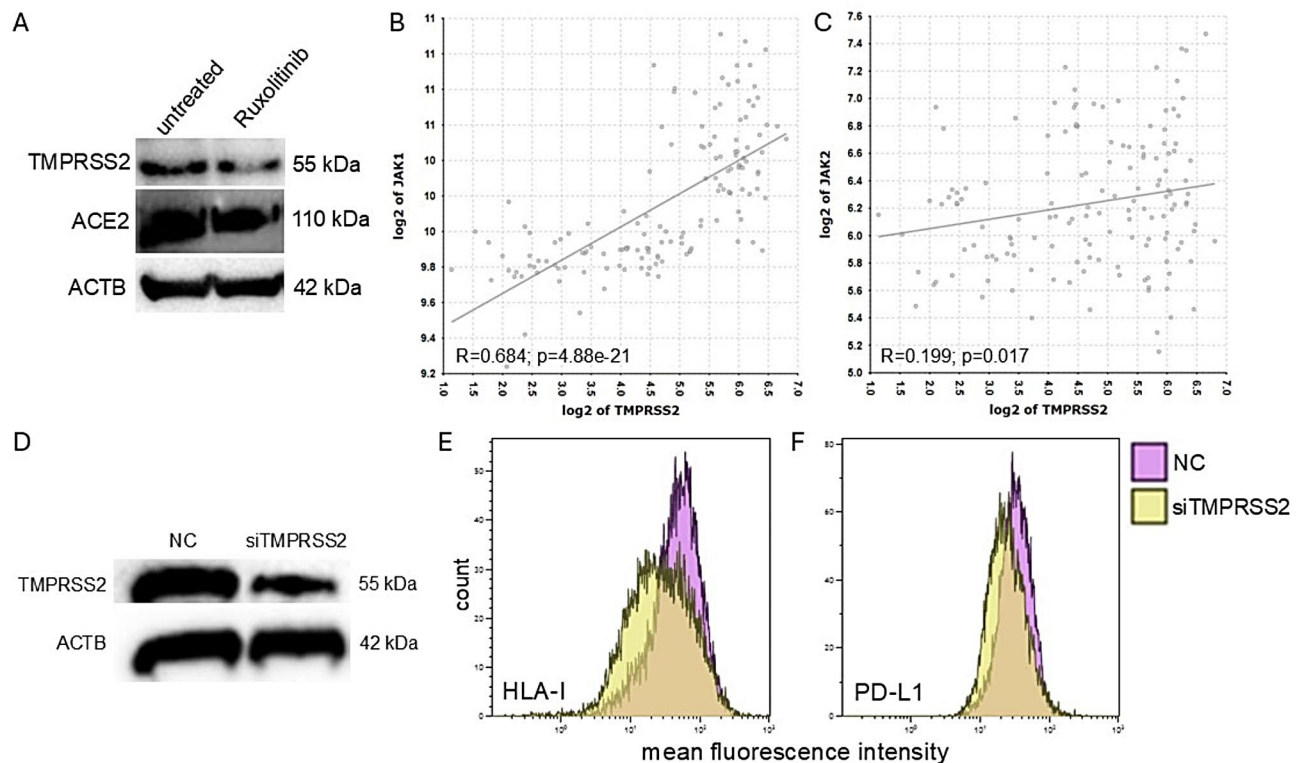


Fig. 6 Decreased TMPRSS2 levels upon ruxolitinib treatment. **A:** Western blot analyses were performed using antibodies targeting TMPRSS2 and ACE2 in cells treated with 300 nM of ruxolitinib. **B, C:** Correlation plots were generated for TMPRSS2 with JAK1 (**B**) and JAK2 (**C**) using the MCF-7 dataset and R2 Genomics. **D:** Reduction of TMPRSS2 by siTMPRSS2 delivered via lipid nanoparticles was evaluated by Western blot analysis with antibodies against TMPRSS2 in MDA-MB-468 cells. **E, F:** Silencing of TMPRSS2 resulted in a significant reduction in HLA-I (**E**) and PD-L1 (**F**) surface expression assessed by flow cytometry

significantly reduced in the presence of $\text{TMPRSS2}^{\text{high}}$ cells upon nivolumab (Fig. 7F). No statistically significant changes of other cytokines were detected in the supernatants of untreated and nivolumab-treated $\text{TMPRSS2}^{\text{high}}$ cells suggesting no interference of ICPi with the cytokine storm (Supplementary Table 6).

Discussion

Patients with cancer are more affected by COVID-19 with longer hospitalization time and increased mortality [8, 43]. So far, the impact of additional treatments affecting the immune system, such as immunotherapy or immunosuppressive agents, on the severity of COVID-19 in tumor patients has not yet been determined [8]. Our study showed that TMPRSS2 affected the expression of the IFN signaling components including JAK-STAT genes in both tumor cell lines and patients' samples, which is consistent with the COVID-19 genome databases (COVID19db; GEO: GSE147507). This is linked to an increased HLA-I and PD-L1 expression suggesting that cancer patients with COVID-19 might respond more to ICPi treatments directed against the PD1/PD-L1 axis (Fig. 8).

Since coronaviruses are considered emerging and re-emerging pathogens [44], anti-viral strategies targeting multiple coronaviruses are urgently needed. High TMPRSS2 expression levels associated with SARS-CoV-2 infection were also frequently found in various cancers. Despite TMPRSS2 as well as ACE2 has higher expression levels after the onset of COVID-19 and cancers [45], no detailed study is available on their expression and interaction in cancer patients infected with COVID-19 or any other coronaviruses. Recently, a correlation between ACE2 expression and immune response has been reported [46], which highlights the potential role of coronavirus target genes in shaping the tumor microenvironment (TME) and influencing tumor behavior during viral infections. The in vitro tumor models investigated in this study showed that TMPRSS2 could enhance ACE2 expression in cancer cells, but an in depth understanding of the precise molecular pathways, through which TMPRSS2 regulates ACE2, requires further investigations.

There exists evidence of an IFN- γ component-mediated control of APM molecules in tumors [47], but APM components have not been extensively studied in the context of COVID-19. Interestingly, an upregulation of

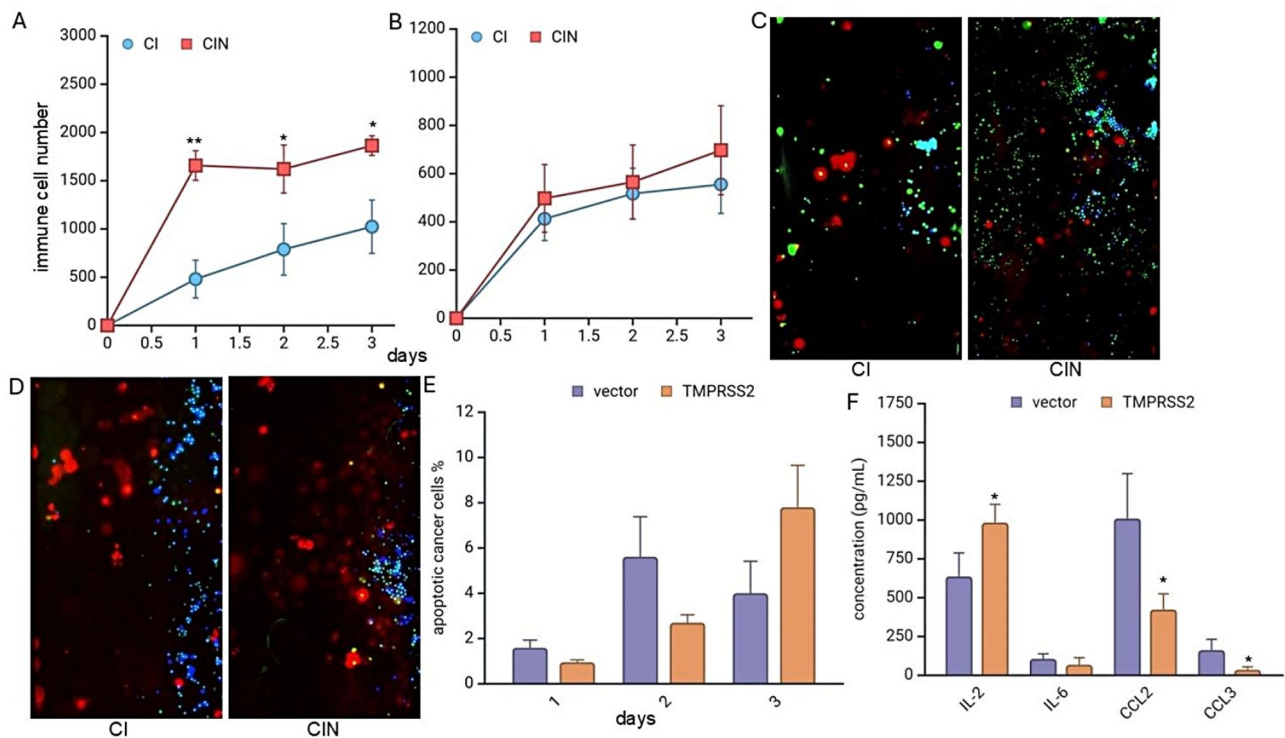


Fig. 7 Microfluidic chip-based analyses of nivolumab-mediated effects on immune cell migration and cytokine release towards TMPRSS2^{high} cells. **A, B:** During a 3-day period, immune cells significantly infiltrated toward TMPRSS2^{high} MCF-7 cells (**A**), but not to TMPRSS2^{low} cells (**B**) treated with nivolumab. **C, D.** Representative immunofluorescent images of day 3 cancer cells, TMPRSS2^{high} (**C**) and TMPRSS2^{low} (**D**) marked in red, lymphocytes in blue and apoptotic cells in green. **E:** Percentage of apoptotic cells of TMPRSS2^{high}/vector MCF-7 cells. Nivolumab therapy on immune cells showed a marginally higher apoptosis rate in TMPRSS2^{high} compared to TMPRSS2^{low} cells. **F:** Higher release of IL-2 and reduced CCL2 and CCL3 levels in TMPRSS2^{high} MCF-7 cells when compared to mock-transfected cells. CI - Cancer cells co-cultured with Immune cells, CIN - CI treated with nivolumab

many APM components, particularly TAP2, was found in TMPRSS2^{high} cells and COVID-19 PBMCs. Furthermore, KEGG pathway analyses indicated an enrichment of several signaling pathways associated with virus infection and the NOD-like receptor signaling in PBMCs of patients with COVID-19 disease [48, 49]. In a multi-cohort study, IFI27 transcription was identified as an early predictor for the outcome of COVID-19 patients [50]. Consistent with these data, our TMPRSS2^{high} EA.Hy926 transfectants showed increased IFI27 mRNA (Log2FC 3.57; p 3.68E-15) and protein levels. IFNs play a dual role in immune responses. They enhance the immune system's ability to eliminate tumor cells, while promoting mechanisms leading to inflammation and allowing immune evasion by e.g. upregulation of PD-L1. The IFN-mediated increase in PD-L1 expression represents a form of "adaptive resistance" [51], which we demonstrated in our results with an upregulation of IFN and PD-L1 in cells with high TMPRSS2 expression and in COVID-19 patients. Furthermore, increased expression of IFN signaling pathway molecules along with IL-6 in long COVID-19 patients indicated a potential role of IFN signaling in the prolonged effects in these patients [35]. Upon binding of IFN to its receptor, JAK kinases

are activated leading to STAT1 phosphorylation [52] and consequently to induction of PD-L1 expression [53]. Interestingly, TMPRSS2^{high} cells expressed high levels of phosphorylated STAT1 thereby triggering PD-L1 surface expression. An improved understanding of the connection between PD-L1 expression and JAK-STAT signaling might provide novel options for combination therapies. The efficacy of PD-1/PD-L1 blockade could be enhanced by the use of JAK inhibitors [51]. Indeed, in patients with Hodgkin lymphoma [54] and in those with non-small cell lung cancer [55], JAK inhibition improved checkpoint blockade immunotherapy. Additionally, JAK inhibitors, such as ruxolitinib, have been discussed for their potential in treating COVID-19 [24, 56] with focus on ACE2. This was extended by our study to TMPRSS2, which is a direct target of ruxolitinib. Elevated levels of the ICP molecule IDO1, alongside PD-L1, in the transcriptome profile of TMPRSS2^{high} and SARS-CoV-2-infected cells were found suggesting exploring the potential application of IDO1 inhibitors.

Growth factors and inflammatory cytokines, such as EGF, IL-6, IFN- γ , TNF- α and TGF- β , can induce PD-L1 expression [57, 58]. However, whether anti-PD-1/PD-L1 treatment would be beneficial for COVID-19 patients has

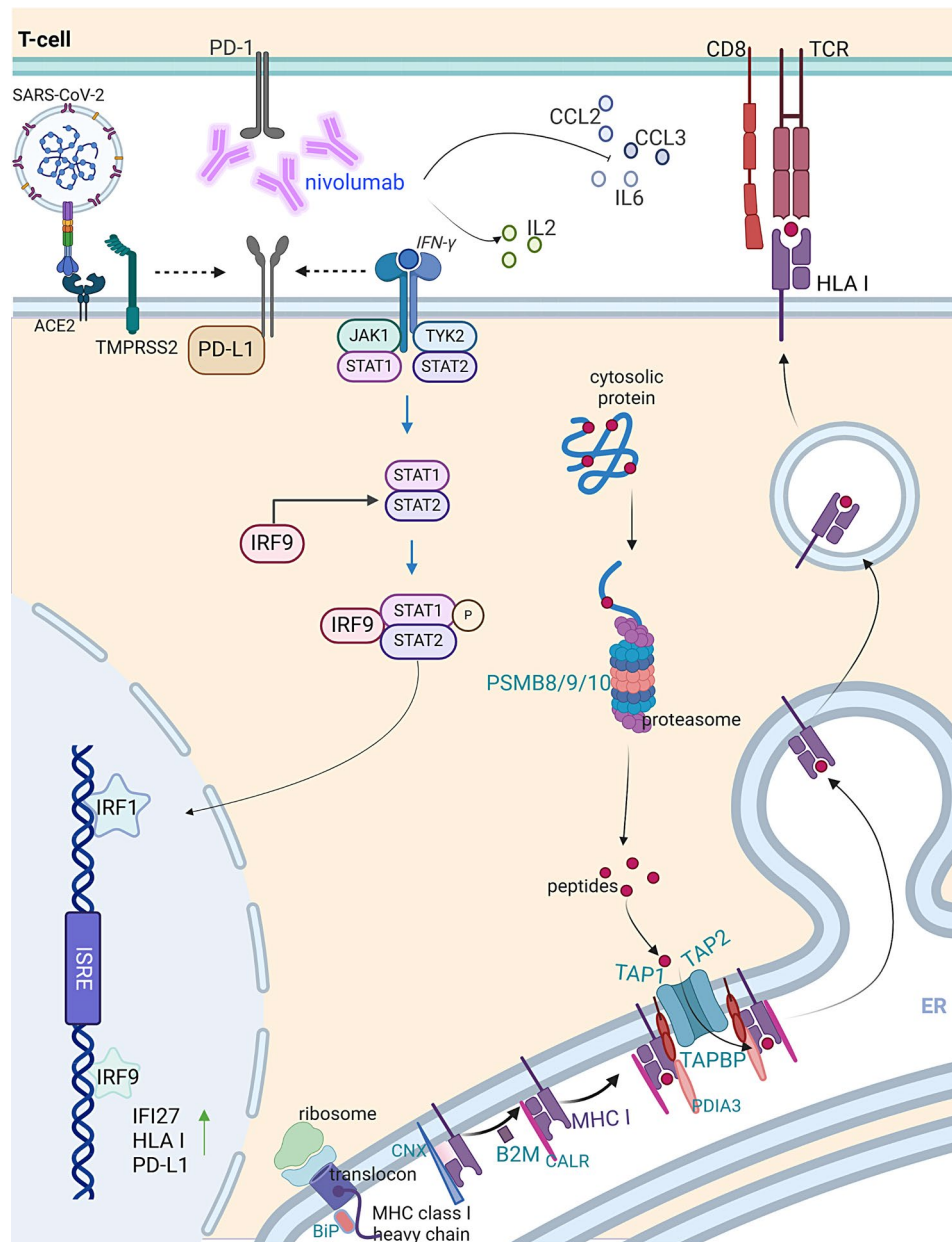


Fig. 8 Cells exhibiting elevated levels of TMPRSS2 demonstrated increased levels of PD-L1, the IFN pathway, HLA class I antigen presentation machinery (APM) and immune responses in comparison to those with lower TMPRSS2 levels. This indicates that the expression of TMPRSS2 across various model systems and following SARS-CoV-2 infection correlates with alterations in host immunogenicity. These alterations may influence the efficacy of the PD-1 inhibitor nivolumab, which enhances the migration of immune cells and decreases cytokines associated with innate immunity (created with BioRender.com)

to be investigated, since this treatment might enhance the cytokine storm associated with higher COVID-19 morbidity and mortality [59, 60]. It is noteworthy that melanoma patients with COVID-19 displayed better outcomes when treated with ICPI [61, 62]. Therefore, anti-PD-1 therapy may also benefit SARS-CoV-2-infected patients. Our data indicates that TMPRSS2^{high} cells, which have increased PD-L1 expression, responded to nivolumab, demonstrating a TMPRSS2-dependent

response along with increased immune cell infiltration into cancer cells.

Cytokines mediate the expansion, activation and trafficking of effector lymphocytes, but can also recruit regulatory T cells [63]. Additionally, TMPRSS2-mediated higher STAT1 expression could regulate IFN- γ -induced CCL2 expression [64]. This decline in CCL2 and CCL3 might revert T cell exclusion and the cytokine storm thereby affecting COVID-19 severity. A decreased

innate immunity and the release of anti-inflammatory cytokines CCL2 and CCL3, respectively, were detected in TMPRSS2 transfectants co-cultured with PBMCs upon nivolumab treatment. Targeting TMPRSS2 with ruxolitinib may reduce its expression and revert the associated immune suppression, while nivolumab could enhance immune cell activity against tumors expressing TMPRSS2. A recent clinical trial demonstrated that ruxolitinib in combination with nivolumab improved the clinical outcome of patients primarily not responding to checkpoint blockade. This result paves the way for novel therapeutic strategies for cancer and COVID-19 patients [54]. On the other hand, further studies are needed to understand how anti-PD-1 therapy affects TMPRSS2, cytokine storm, IFN signaling and lymphocyte composition and function following SARS-CoV-2 infection.

Conclusions

Our research indicates a link between TMPRSS2 and different types of tumors as well as an effect of SARS-CoV-2 infection on the immune response by activating immune-related pathways. Targeting TMPRSS2 as a universal coronavirus strategy shows potential for the design of novel treatments and vaccines that can offer broad protection against current and future coronavirus threats. Our study emphasizes the importance of using in vitro disease models and RNA-seq datasets to form hypotheses relevant to human disease. Our findings show that treatment with an anti-PD-1 antibody improved the infiltration of immune cells and inhibited the production of inflammatory cytokines in an in vitro TMPRSS2^{high} model. These results suggest that anti-PD-L1 treatment could restrict T cell exhaustion and hinder virus infectivity at an early stage of virus entry. Combining TMPRSS2 inhibitors with immune modulators, such as PD-1 inhibitors and/or JAK inhibitors, may offer a comprehensive approach for the treatment of COVID-19, but the therapeutic strategies need to be balanced between enhancing anti-viral immunity and preventing excessive inflammation and activation of the immune system, which can cause tissue damage and worsen outcomes as observed in severe COVID-19 cases.

Abbreviations

2D	Two dimensional
3D	Three dimensional
Ab	Antibody
ACE2	Angiotensin-converting enzyme-2
APM	Antigen processing machinery
ATCC	American Type Culture Collection
BC	Breast cancer
β2-m	β2-microglobulin
BP	Biological process
BC	Breast cancer
CC	Cellular component
CoV	Coronavirus
CRC	Colorectal carcinoma
CSF	Colony stimulating factor

DEG	Differentially expressed gene
DGE	Differential gene expression
DSS	Disease-specific survival
FCS	Fetal calf serum
FDR	False discovery rate
GADPH	Glyceride aldehyd-3-phosphate dehydrogenase
GO	Gene ontology
HC	Heavy chain
HLA	Human leukocyte antigen
HRP	Horse reddish peroxidase
ICP	Immune checkpoint
ICPi	Immune checkpoint inhibitor
IDO	Indoleamine 2,3-dioxygenase
IFN	Interferon
IL	Interleukin
KEGG	Kyoto Encyclopedia of Genes and Genomes
LMP	Low molecular weight protein
LNP	Lipid nanoparticles
mAb	monoclonal antibody
MAS	Macrophage activation syndrome
MCP-1	Monocyte chemoattractant protein-1
MF	Molecular function
MFI	Mean fluorescence intensity
MHC	Major histocompatibility complex
MIP-1α	Macrophage inflammatory protein 1 alpha
NK	Natural killer
OS	Overall survival
PBMC	Peripheral blood mononuclear cells
PD1	Programed death receptor 1
PD-L1	Programed death ligand 1
S	Spike
SARS	Severe acute respiratory syndrome
TAP	Transporter associated with antigen processing
TCGA	The Cancer Genome Atlas
TGF-β	transforming growth factorβ
TME	Tumor microenvironment
TMPRSS2	Transmembrane protease, serine 2TNF, tumor necrosis factor
TNF	Tumor necrosis factor
TAPBP	Tapasin

Supplementary Information

The online version contains supplementary material available at <https://doi.org/10.1186/s12967-025-06177-z>.

Supplementary Material 1

Acknowledgements

We thank Maria Heise and Sandra Wolf for their excellent secretarial help and Bo Yang and Helene Schäfer for their initial experimental support.

Author contributions

Karthikeyan Subbarayan contributed to the study's design, experimental analysis, data interpretation, statistics, and writing of the original draft. Helena Bieber performed the transfection experiments, qPCR analysis, Western blot analysis and flow cytometry. Felipe Adonis Escalona Rodríguez and Sandy Tretbar contributed to the LNP preparation and delivery. Chiara Massa performed the NK cell assays. SM Al Amin Hossain and Karthikeyan Subbarayan performed bioinformatic analysis. Lisa Neuder performed a qPCR analysis. Ahmed Al-Samadi, Tuula Salo, and Wafa Wahbi conducted the microfluidic chip assay. Barbara Seliger was involved in conceptualization, funding acquisition, investigation, supervision, and writing, review & editing of the manuscript. All authors reviewed and approved the final version of the manuscript.

Funding

Open Access funding enabled and organized by Projekt DEAL. This study was financially supported from the following organizations: DAAD (GLACIER-project of the German Federal Foreign Ministry, project-ID 57592717), Deutsche Forschungsgemeinschaft (DFG, SE 581/33 – 1), State of Lower

Saxony (LSA COVID grants, FKZ: I 234, I 200, I 152), Research Council of Finland, Sigrid Jusélius Foundation, and Minerva Foundation.

Data availability

All data generated or analyzed during this study are included either in this article or in the supplementary information files. The datasets generated during and/or analyzed during the current study are available from the corresponding author upon reasonable request.

Declarations

Ethical approval

Ethical approval for this study was obtained from the Finnish Red Cross and the MLU for the usage of PBMNC in this study. All other datasets used in this work are obtained from public databases and are freely available. This work did not include any experiments on humans or animals. The patients involved in the public databases have been enrolled after ethical approval and deemed exempt for ethical approval.

Consent for publication

All authors read the final version of the manuscript and gave consent for publication.

Competing interests

The authors declare that the research was conducted in the absence of any commercial or financial relationships that could be construed as a potential conflict of interest.

Author details

¹Medical Faculty, Martin Luther University Halle-Wittenberg, Halle (Saale), Germany

²Institute of Translational Immunology, Faculty of Health Sciences, Brandenburg Medical School "Theodor Fontane", Brandenburg an der Havel, Germany

³Center for Protein Studies, Faculty of Biology, University of Havana (UH), Havana, Cuba

⁴NanoCancer, Molecular Immunology Center (CIM), Havana, Cuba

⁵Department of Oral and Maxillofacial Diseases, Clinicum, University of Helsinki, Helsinki, Finland

⁶Cancer and Translational Medicine Research Unit, University of Oulu, Oulu 90014, Finland

⁷Fraunhofer Institute for Cell Therapy and Immunology, Leipzig, Germany

⁸Institute of Dentistry, School of Medicine, Faculty of Health Sciences, University of Eastern Finland, Kuopio, Finland

Received: 2 January 2025 / Accepted: 24 January 2025

Published online: 07 March 2025

References

- Rahman N et al. Virtual screening of Natural products against type II transmembrane serine protease (TMPRSS2), the Priming Agent of Coronavirus 2 (SARS-CoV-2). *Molecules*. 2020. 25(10).
- Thunders M, Delahunt B. Gene of the month: TMPRSS2 (transmembrane serine protease 2). *J Clin Pathol*. 2020;73(12):773–6.
- Hoffmann M, et al. SARS-CoV-2 cell entry depends on ACE2 and TMPRSS2 and is blocked by a clinically proven protease inhibitor. *Cell*. 2020;181(2):271–e2808.
- Huggins DJ. Structural analysis of experimental drugs binding to the SARS-CoV-2 target TMPRSS2. *J Mol Graph Model*. 2020;100:107710.
- Shen LW, et al. TMPRSS2: a potential target for treatment of influenza virus and coronavirus infections. *Biochimie*. 2017;142:1–10.
- Kuderer NM, et al. Clinical impact of COVID-19 on patients with cancer (CCC19): a cohort study. *Lancet*. 2020;395(10241):1907–18.
- Rivera DR, et al. Utilization of COVID-19 treatments and clinical outcomes among patients with Cancer: a COVID-19 and Cancer Consortium (CCC19) cohort study. *Cancer Discov*. 2020;10(10):1514–27.
- Bakouny Z, et al. Interplay of Immunosuppression and Immunotherapy among patients with Cancer and COVID-19. *JAMA Oncol*. 2023;9(1):128–34.
- Nie L, et al. Clinical characteristics and risk factors for in-hospital mortality of lung cancer patients with COVID-19: a multicenter, retrospective, cohort study. *Thorac Cancer*. 2021;12(1):57–65.
- Cacuri F, Caruso A. Endothelial cells are major players in SARS-CoV-2-related acute respiratory distress syndrome. *EBioMedicine*. 2022;86:104328.
- Fedeli U, et al. Changes in cancer-related mortality during the COVID-19 pandemic in the United States. *J Natl Cancer Inst*. 2024;116(1):167–9.
- Zhao J, et al. Association of the COVID-19 pandemic and changes in patterns of Cancer-related mortality in the United States. *JCO Oncol Pract*. 2023;19(7):501–8.
- Subbarayan K, et al. Immune Interaction Map of Human SARS-CoV-2 target genes: implications for therapeutic avenues. *Front Immunol*. 2021;12:597399.
- Razaghi A et al. Proteomic Analysis of Pleural Effusions from COVID-19 deceased patients: enhanced inflammatory markers. *Diagnostics (Basel)*, 2022. 12(11).
- Sabbatino F, et al. PD-L1 dysregulation in COVID-19 patients. *Front Immunol*. 2021;12:695242.
- Mei Q et al. Impact of COVID-19 vaccination on the use of PD-1 inhibitor in treating patients with cancer: a real-world study. *J Immunother Cancer*, 2022. 10(3).
- Subbarayan K, et al. Expression and clinical significance of SARS-CoV-2 human targets in neoplastic and non-neoplastic lung tissues. *Curr Cancer Drug Targets*. 2021;21(5):428–42.
- Cao W, Feng Q, Wang X. Computational analysis of TMPRSS2 expression in normal and SARS-CoV-2-infected human tissues. *Chem Biol Interact*. 2021;346:109583.
- Lucas JM, et al. The androgen-regulated protease TMPRSS2 activates a proteolytic cascade involving components of the tumor microenvironment and promotes prostate cancer metastasis. *Cancer Discov*. 2014;4(11):1310–25.
- Xiao X, et al. TMPRSS2 serves as a prognostic biomarker and correlated with Immune infiltrates in breast Invasive Cancer and Lung Adenocarcinoma. *Front Mol Biosci*. 2022;9:647826.
- Niri P, et al. Role of biomarkers and molecular signaling pathways in acute lung injury. *Fundam Clin Pharmacol*. 2024;38(4):640–57.
- Prieto Santamaria L, et al. Integrating heterogeneous data to facilitate COVID-19 drug repurposing. *Drug Discov Today*. 2022;27(2):558–66.
- Seliger B, Ruiz-Cabello F, Garrido F. IFN inducibility of major histocompatibility antigens in tumors. *Adv Cancer Res*. 2008;101:249–76.
- Goker Bagca B, Biray C, Avci. The potential of JAK/STAT pathway inhibition by ruxolitinib in the treatment of COVID-19. *Cytokine Growth Factor Rev*. 2020;54:51–62.
- Bukur J, et al. Identification of E2F1 as an important transcription factor for the regulation of tapasin expression. *J Biol Chem*. 2010;285(40):30419–26.
- Meyer S et al. Distinct molecular mechanisms of altered HLA class II expression in malignant melanoma. *Cancers (Basel)*, 2021. 13(15).
- Mortazavi A, et al. Mapping and quantifying mammalian transcriptomes by RNA-Seq. *Nat Methods*. 2008;5(7):621–8.
- Sievilainen M, et al. IDO1 inhibition reduces Immune Cell Exclusion through Inducing Cell Migration while PD-1 blockage increases IL-6 and -8 secretion from T cells in Head and Neck Cancer. *Front Immunol*. 2022;13:812822.
- Thair SA, et al. Transcriptomic similarities and differences in host response between SARS-CoV-2 and other viral infections. *iScience*. 2021;24(1):101947.
- Zhang W, et al. COVID19db: a comprehensive database platform to discover potential drugs and targets of COVID-19 at whole transcriptomic scale. *Nucleic Acids Res*. 2022;50(D1):D747–57.
- Ziegler CGK, et al. SARS-CoV-2 receptor ACE2 is an Interferon-stimulated gene in human airway epithelial cells and is detected in specific cell subsets across tissues. *Cell*. 2020;181(5):1016–e103519.
- Blanco-Melo D, et al. Imbalanced host response to SARS-CoV-2 Drives Development of COVID-19. *Cell*. 2020;181(5):1036–e10459.
- Daamen AR, et al. Comprehensive transcriptomic analysis of COVID-19 blood, lung, and airway. *Sci Rep*. 2021;11(1):7052.
- Wilk AJ, et al. A single-cell atlas of the peripheral immune response in patients with severe COVID-19. *Nat Med*. 2020;26(7):1070–6.
- Yin K, et al. Long COVID manifests with T cell dysregulation, inflammation and an uncoordinated adaptive immune response to SARS-CoV-2. *Nat Immunol*. 2024;25(2):218–25.
- Solstad AD et al. IFN-lambda uniquely promotes CD8 T cell immunity against SARS-CoV-2 relative to type I IFN. *JCI Insight*, 2024. 9(13).
- Chandrashekar DS, et al. An update to the integrated cancer data analysis platform. *Neoplasia*. 2022;25:18–27.

38. Chandrashekar DS, et al. A portal for facilitating Tumor Subgroup Gene expression and survival analyses. *Neoplasia*. 2017;19(8):649–58.
39. Liu J, et al. An Integrated TCGA Pan-cancer Clinical Data Resource to Drive High-Quality Survival Outcome Analytics. *Cell*. 2018;173(2):400–e41611.
40. Broman N, et al. IL-6 and other biomarkers as predictors of severity in COVID-19. *Ann Med*. 2021;53(1):410–2.
41. Mesa RA. Ruxolitinib, a selective JAK1 and JAK2 inhibitor for the treatment of myeloproliferative neoplasms and psoriasis. *IDrugs*. 2010;13(6):394–403.
42. Loretelli C et al. PD-1 blockade counteracts post-COVID-19 immune abnormalities and stimulates the anti-SARS-CoV-2 immune response. *JCI Insight*, 2021;6(24).
43. Bakouny Z, et al. COVID-19 and Cancer: current challenges and perspectives. *Cancer Cell*. 2020;38(5):629–46.
44. Cheng VC, et al. Severe acute respiratory syndrome coronavirus as an agent of emerging and reemerging infection. *Clin Microbiol Rev*. 2007;20(4):660–94.
45. Liu C, et al. High expression of ACE2 and TMPRSS2 and clinical characteristics of COVID-19 in colorectal cancer patients. *NPJ Precis Oncol*. 2021;5(1):1.
46. Subbarayan K, et al. Altered ACE2 and interferon landscape in the COVID-19 microenvironment correlate with the anti-PD-1 response in solid tumors. *Cell Mol Life Sci*. 2024;81(1):473.
47. Seliger B, et al. Coordinate downregulation of multiple MHC class I antigen processing genes in chemical-induced murine tumor cell lines of distinct origin. *Tissue Antigens*. 2000;56(4):327–36.
48. Almeida-da-Silva CLC, et al. The role of NOD-like receptors in innate immunity. *Front Immunol*. 2023;14:1122586.
49. Lei X, et al. Activation and evasion of type I interferon responses by SARS-CoV-2. *Nat Commun*. 2020;11(1):3810.
50. Shojaei M, et al. IFI27 transcription is an early predictor for COVID-19 outcomes, a multi-cohort observational study. *Front Immunol*. 2022;13:1060438.
51. Benci JL, et al. Tumor Interferon Signaling regulates a multigenic resistance program to Immune Checkpoint Blockade. *Cell*. 2016;167(6):1540–e155412.
52. Holzgruber J, et al. Type I interferon signaling induces melanoma cell-intrinsic PD-1 and its inhibition antagonizes immune checkpoint blockade. *Nat Commun*. 2024;15(1):7165.
53. Mimura K, et al. PD-L1 expression is mainly regulated by interferon gamma associated with JAK-STAT pathway in gastric cancer. *Cancer Sci*. 2018;109(1):43–53.
54. Zak J, et al. JAK inhibition enhances checkpoint blockade immunotherapy in patients with Hodgkin lymphoma. *Science*. 2024;384(6702):ead8520.
55. Mathew D, et al. Combined JAK inhibition and PD-1 immunotherapy for non-small cell lung cancer patients. *Science*. 2024;384(6702):eadf1329.
56. Vannucchi AM, et al. Compassionate use of JAK1/2 inhibitor ruxolitinib for severe COVID-19: a prospective observational study. *Leukemia*. 2021;35(4):1121–33.
57. Zhang W et al. IL-6 promotes PD-L1 expression in monocytes and macrophages by decreasing protein tyrosine phosphatase receptor type O expression in human hepatocellular carcinoma. *J Immunother Cancer*, 2020. 8(1).
58. Huang HC, et al. Upregulation of PD-L1 by SARS-CoV-2 promotes immune evasion. *J Med Virol*. 2023;95(2):e28478.
59. Gillissen S, Powles T. Advice regarding systemic therapy in patients with urological cancers during the COVID-19 pandemic. *Eur Urol*. 2020;77(6):667–8.
60. Postow MA, Sidlow R, Hellmann MD. Immune-related adverse events Associated with Immune Checkpoint Blockade. *N Engl J Med*. 2018;378(2):158–68.
61. Moritz RKC, et al. SARS-CoV-2 infections in melanoma patients treated with PD-1 inhibitors: a survey of the German ADOREG melanoma registry. *Eur J Cancer*. 2021;144:382–5.
62. Isgro MA, et al. Immunotherapy may protect cancer patients from SARS-CoV-2 infection: a single-center retrospective analysis. *J Transl Med*. 2021;19(1):132.
63. Berraondo P, et al. Cytokines in clinical cancer immunotherapy. *Br J Cancer*. 2019;120(1):6–15.
64. Penrose HM, et al. STAT1 regulates interferon-gamma-induced angiotensinogen and MCP-1 expression in a bidirectional manner in primary cultured mesangial cells. *J Renin Angiotensin Aldosterone Syst*. 2020;21(3):1470320320946527.

Publisher's note

Springer Nature remains neutral with regard to jurisdictional claims in published maps and institutional affiliations.